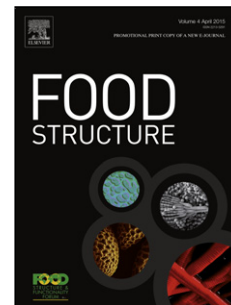


Accepted Manuscript

Title: Physical and Interfacial Characterization of Phytosterols in Oil-in-Water Triacylglycerol-Based Emulsions

Authors: Lisa M. Zychowski, Srinivas Mettu, Raymond R. Dagastine, Alan L. Kelly, James A. O'Mahony, Mark A.E. Auty



PII: S2213-3291(18)30016-9
DOI: <https://doi.org/10.1016/j.foostr.2018.11.001>
Reference: FOOSTR 101

To appear in:

Received date: 16 February 2018
Revised date: 1 November 2018
Accepted date: 14 November 2018

Please cite this article as: Zychowski LM, Mettu S, Dagastine RR, Kelly AL, O'Mahony JA, Auty MAE, Physical and Interfacial Characterization of Phytosterols in Oil-in-Water Triacylglycerol-Based Emulsions, *Food Structure* (2018), <https://doi.org/10.1016/j.foostr.2018.11.001>

This is a PDF file of an unedited manuscript that has been accepted for publication. As a service to our customers we are providing this early version of the manuscript. The manuscript will undergo copyediting, typesetting, and review of the resulting proof before it is published in its final form. Please note that during the production process errors may be discovered which could affect the content, and all legal disclaimers that apply to the journal pertain.

**Physical and Interfacial Characterization of Phytosterols in Oil-in-Water
Triacylglycerol-Based Emulsions**

Lisa M. Zychowski^{†§}, Srinivas Mettu^{#‡}, Raymond R. Dagastine^{#‡}, Alan L. Kelly[§], James A.
O'Mahony[§], Mark A. E. Auty^{*†}

[†] Food Chemistry and Technology Department, Teagasc Food Research Centre, Moorepark,
Fermoy, Co. Cork, Ireland

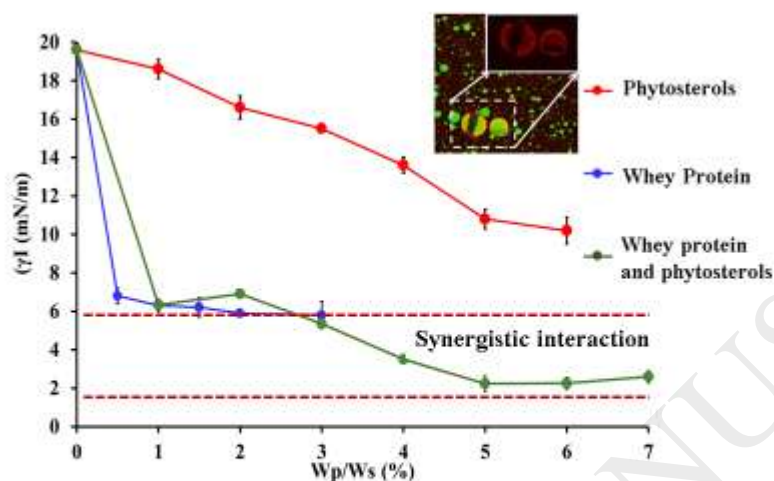
[§] School of Food and Nutritional Sciences, University College Cork, Cork, Ireland

[#] Department of Chemical Engineering, Parkville, Victoria, Australia

[‡] Particulate Fluids Processing Centre (PFPC), Parkville, Victoria, Australia

*Corresponding author (M.A.E.A) address: Mondelez International, Reading Science Centre,
Reading, UK, Tel: 44 (0) 1189 450542, email: mark.auty@mdlz.com.

Graphical abstract



Highlights

- Phytosterols can crystallise within an oil and water-based emulsion system and can influence emulsion surface morphology.
- Phytosterols are able to lower interfacial tension at an oil and water interface.
- The combination of phytosterols and whey protein was able to lower interfacial tension to a greater extent than the two components separately.
- A synergistic interaction between phytosterols and whey protein was proposed and confirmed by interfacial modeling.

Abstract: Phytosterols possess the ability to significantly lower low-density lipoprotein (LDL) cholesterol levels in the blood, but their bioaccessibility is highly dependent upon the solubility

of the phytosterol within the carrier matrix. Currently, there is a limited amount of knowledge on how phytosterols interact at oil-water interfaces, despite research indicating that these interfaces could promote the crystallization of phytosterols and thus decrease bioaccessibility. In order to fill this knowledge gap, this work expands upon a previously studied emulsion system for encapsulating phytosterols and addresses whether phytosterols can crystallize at an oil-in-water emulsion interface. Images from multiple microscopic techniques suggest interfacial phytosterol crystallization in 0.6% phytosterol-enriched emulsions, while interfacial tension results and calculated models showed that whey protein and phytosterols had a synergistic effect on interfacial tension. A deeper understanding of the interfacial behavior of phytosterols in emulsions can provide the functional food and pharmaceutical industry with the knowledge needed to design more bioaccessible phytosterol-enriched products.

Abbreviations: CSLM-Confocal laser scanning microscopy, Cryo-SEM-Cryo-scanning electron microscopy MCT-Medium-chain triglyceride, PLM-polarized light microscopy

Keywords: phytosterols, plant sterols, β -sitosterol, LDL cholesterol, functional foods, interfacial tension, emulsion, bioactive, microscopy

ACCEPTED MANUSCRIPT

1. Introduction

Phytosterols, or plant sterols, are compounds found within plant-cell membranes that are well-known for their ability to reduce levels of low-density lipoprotein (LDL) cholesterol in the blood (Jones, MacDougall, Ntanios, & Vanstone, 1997; Moruise, Oosthuizen, & Opperman, 2006; Ostlund, 2002). Phytosterols are present in all foods of plant origins, such as fruits, cereals, and nuts, but only in limited concentrations. To significantly lower LDL-cholesterol levels, dietary supplementation is needed to achieve the recommended > 1.5 g of phytosterols per day (Berger, Jones, & Abumweis, 2004). Therefore, as the incidence of heart disease increases and consumers become more health-conscious, so does the use of phytosterols within food products (Henson, Cranfield, & Herath, 2010; Zawistowski, 2010). Phytosterol-enriched food products, or functional foods, can be utilized to lower cholesterol levels simply by regularly ingesting the food product. Despite their increased use within the functional food sector, little is known about how phytosterols interact with different food components.

On a molecular level, phytosterols are chemically similar to human cholesterol and possess the same tetracyclic-backbone; differences between the two compounds arise at the C-22 and C-5 positions, with the presence or absence of various side chains and/or a double bond. These various side chains also distinguish between phytosterol varieties, the most common being β -sitosterol, stigmasterol and campesterol (Jones & AbuMweis, 2009; Ostlund, 2002). The molecular similarities between phytosterols and human cholesterol enable phytosterols to successfully reduce serum cholesterol levels by preventing cholesterol absorption within the small intestine (Santas, Codony, & Rafecas, 2013). Phytosterols also possess anti-

inflammatory and anti-carcinogenic properties and have no associated negative side-effects (Engel & Schubert, 2005; Jones et al., 1997).

Despite these benefits, phytosterol enrichment of food systems is not common due to formulation difficulties associated with their insolubility and crystallinity at room temperature (Zawistowski, 2010). Thus, phytosterols are commonly esterified by the industry to improve their solubility and dispersibility within food matrices, such as margarine (Clifton, 2007). Additionally esterification results in higher processing costs, as compared to using natural phytosterols and unpredictable absorption rates (Clifton, 2007). Phytosterol esters have to be hydrolyzed prior to absorption, which is subject to inter-individual variability among human digestive systems, resulting in absorption rates varying between 40-96% (Carden, Hang, Dussault, & Carr, 2015).

Conversely, emulsion-based delivery systems can be utilized to enhance the solubility of non-esterified phytosterols, but the bioaccessibility of the emulsion is dependent upon the physical state of the phytosterol (Ostlund, 2002). Previous studies have demonstrated that crystalline, non-solubilized phytosterols are not as effective at lowering LDL-cholesterol in the blood, as solubilized phytosterols (Jones & AbuMweis, 2009; Pouteau et al., 2003). Phytosterols can crystallize within the carrier oil, but it should be noted that the presence of water at the interface can also induce sterol crystallization (Engel & Schubert, 2005; Jandacek, Webb, & Mattson, 1977). Phytosterols possess the ability to lower interfacial tension, and thus their propensity to move to an interface could lead to crystallization and decreased bioaccessibility (Cercaci, Rodriguez-Estrada, Lercker, & Decker, 2007).

Despite phytosterol crystallization resulting in decreased bioaccessibility in functional food emulsions, very little research has been performed in analysing the mechanism by which phytosterols crystallize. Previously research conducted by the group highlighted how

phytosterols crystallize within a triacylglycerol-based food emulsion, utilizing whey protein as the emulsifier; however, little emphasis was placed upon the possibility of phytosterol crystallization at the interface (Zychowski et al., 2016). Thus, this work seeks to investigate the possibility of phytosterols crystallization at the interface and to characterize how phytosterols influence the morphology and physical properties of a food emulsion. The morphology of phytosterol-enriched emulsions (PE emulsions) were analyzed utilizing confocal laser scanning microscopy, cryo-scanning electron microscopy, polarized light microscopy, and a Malvern mastersizer to study droplet size distribution. Interfacial tension and modelling were used to understand phytosterol and whey protein behavior at the emulsion interface. By understanding how the interfacial behavior of phytosterols influences the properties of a food emulsion, the functional food industry can design more stable and bioaccessible, phytosterol-enriched products.

2. Materials and Methods

2.1 Chemicals and Ingredients

Crystalline phytosterols, glycerol, and sodium azide were purchased from Sigma Aldrich (Wicklow, Ireland). The main sterol present was β -sitosterol ($\geq 70\%$) with residual campesterol and β -sitostanol. Commercial-grade anhydrous milk fat (AMF) was obtained from Cormac Miloko (Tipperary, Ireland). Whey protein isolate (WPI; BiPro®, of 92.7% protein) was purchased from Davisco Foods International Inc (Minnesota, USA). Purified medium-chain triglyceride oil was procured from Pure Vita labs (British Columbia, Canada) for interfacial measurements.

2.2 Preparation of Emulsions

Oil-in-water emulsions (10% oil: 1% protein: 89% H₂O) were prepared on a wt/wt basis with or without added phytosterols in the oil ratio (0.3% or 0.6% wt/wt) as detailed by Zychowski

et al. (2016). Emulsions were prepared by homogenization with an APV 1000 homogenizer (SPX flow, Germany) at 300 bar pressure for 1 pass at 60°C. Higher pressures or more passes were not employed within this study as more intense treatments yielded smaller droplets, which were unsuitable for microscopic evaluation (Zychowski et al., 2018). Emulsions were allowed to statically cool and were stored at 20-25°C with 0.1% sodium azide added to the final emulsion. PE emulsions were formulated at levels of 0.0%, 0.3%, and 0.6% (wt/wt) PE with 0.0% functioning as the control. The 0.6% PE sample contained the highest level of phytosterols, as PE emulsions created with 0.8% phytosterols were not stable and separated immediately upon pre-homogenisation. All evaluations and images were carried out within 24 h on samples from three separate emulsion trials.

2.3 Physical Characterization of Emulsions

2.3.1 Particle Size.

The droplet size distribution of the emulsion was measured at 22°C utilizing a Malvern Mastersizer 3000 equipped with a Hydro R cell (Malvern Instruments Ltd, Worcestershire, UK). Distilled water was used as the dispersing medium with an obscuration between 4-10% and absorption level of 0.001. Refractive index values of 1.33 for water and 1.46 for milk fat were used in the optical parameters. The $D_{(4,3)}$ value was calculated by the Mastersizer 3000 software based on a spherical geometry, where n_i is the number of droplets with diameter d_i (eq 1). All evaluations were carried out in triplicate on three separate emulsion trials.

$$D_{4,3} = \left(\sum n_i d_i^4 / \sum n_i d_i^3 \right) \quad (1)$$

2.3.2 Polarized Light Microscopy

Polarized light images were captured using an Olympus BX51 microscope (Olympus Corporation, Tokyo, Japan) at 60X using a ProgRes CT3 camera with Prores 2.7.7 software

(Jenoptik, Wiltshire, UK). Fifty microliters of emulsion samples were placed onto a glass slide with a coverslip. The glass slide was then placed directly onto the heating element of a Linkam LNP heating/cooling stage (Linkam, Surrey, UK). Images were taken at 20°C and after heating to 50°C at 3°C/min since 50°C is above the melting point of milk fat but not of phytosterols within a TAG matrix (Acevedo & Franchetti, 2016; Lopez, Bourgaux, Lesieur, & Ollivon, 2007). Images were taken to characterise changes in emulsion morphology and the presence of crystals above the melting point of milk fat.

2.3.3 Confocal Laser Scanning Microscopy

Imaging was performed with a confocal laser scanning microscope (CLSM; Leica Microsystems CMS GmbH, Wetzlar, Germany) with a 63x oil immersion objective and 3x and 5x zoom factors. Samples were prepared for microscopic analysis by adding 10 µl of Nile Blue (Sigma Aldrich, Wicklow) concentrated at 0.1 g/100 µl to 1 ml of emulsion sample and vortexing the sample for 10 s, as detailed previously (Zychowski et al., 2016). Nile blue is used to stain the protein phase and the oxidation product of Nile blue, Nile red, stains the lipid phase (Auty et al., 2001). Nile blue has been found not to influence lipid crystallisation (Herrera & Hartel, 2000). After vortexing, 50 µl of the emulsion was pipetted onto a glass microscope slide and a coverslip was placed on top. Images were captured at 8-bit, 512x512 pixels resolution and were pseudo-colored to show protein (red) and lipid (green). Dual channel confocal imaging employing an Argon laser at 488 nm (Nile red) and a Helium/Neon laser at 633 nm (Nile blue) was used to excite the lipid and protein dyes, respectively. After imaging, the protein and lipid channels were visualised separately and combined to highlight visualization of the protein coverage around the emulsion droplets using the LAS AF software (Leica Microsystems CMS GmbH, Wetzlar, Germany).

2.3.4 Cryo-scanning Electron Microscopy

Cryo-scanning electron microscopy was performed using a Zeiss Supra 40VP field emission SEM (Carl Zeiss SMT Ltd., Cambridge, UK). Samples were prepared for imaging by adding 200 μ l glycerol (cryo-protectant) into 1 ml of emulsion and vortexing for 10 s. Samples were then centrifuged for 5 min at 10,000 rpm in an Eppendorf centrifuge (model 5417R; Eppendorf, Hauppauge, New York) at 20°C to concentrate the fat droplets. Afterwards, 400 μ l of the solution was removed from the top of the tube and mounted onto a slotted aluminum sample holder. In order to cryo-fix the sample, the stage was then plunged immediately into melting liquid nitrogen slush (-210°C). The sample was then transferred under vacuum to the cryo-preparation chamber using the Alto 2500 cryo-transfer device (Gatan Ltd., Oxford, UK). Once inside the chamber, the sample was fractured at -195°C , followed by sublimation at -90°C for 2 min. After sublimation, the sample was sputter-coated with platinum at -130°C and transferred to the cold stage for imaging at -125°C . Secondary electron images were obtained at an operating distance of 6 mm and an accelerating voltage of 2 kV.

2.4 Interfacial and Surface Characterization of Emulsion Systems

2.4.1 Dynamic Interfacial Tension Measurements

Interfacial tension (γ I) was measured using a Kruss K12 tensiometer (Kruss GmbH, Hamburg, Germany) equipped with a Wilhelmy plate, as described previously (Drapala, Auty, Mulvihill, & O'Mahony, 2015). Dynamic (γ I) data was collected continuously during the first 5 min at 60°C and in subsequent 5 min intervals over 30 min; this was performed to simulate emulsion formation conditions and to capture initial changes in (γ I) with the addition of phytosterols and whey proteins at the oil-water interface, respectively. In addition, previous research has demonstrated that phytosterols are in a liquid lamellar state at 60°C in MCT-based

system (Zychowski et al., 2016). Whey protein solutions were reconstituted at 0.5%, 1%, 2%, or 3% (wt/wt; % protein) in an ice bath with Milli-Q water and stirred at 300 rpm. Solutions were then stored overnight at 4°C to allow for complete hydration. Phytosterols were added to the oil phase of MCT at 1% increments between 0.0-6.0% wt/wt as described previously (Zychowski et al., 2016). Filtered water (Milli-Q system) with MCT (no WPI), without phytosterol, was used as a control sample.

Purified MCT oil was used to simulate melted AMF in these emulsions, as the commercial grade AMF used in this study produced inconsistent results between the water and lipid phase, most likely due to the presence of minor lipid components such as phospholipids and free fatty acids. MCT oil was chosen as it has been used previously to study the behaviour of milk proteins in other model milk systems (Waninge et al., 2005).

Before each measurement, the Wilhelmy plate was calibrated by submerging the plate within the light phase, consisting of MCT solution with or without phytosterol. After calibration, 25 ml of the heavy phase, water or whey protein solution, was added into the sample holder. The Wilhelmy plate was then lowered onto the interface and the light phase was added until the plate was completely submerged. The glass sample vessel and Wilhelmy plate were cleaned and annealed before each measurement. All glassware for sample preparation was acid-washed overnight with 1 M Nitric acid and washed 3 times with distilled water before drying. Measurements were completed in triplicate on each interface.

2.4.2. Surface Modeling

In order to describe the interfacial interactions of the phytosterol and WPI interfaces at 60°C, collected interfacial tension data was fitted utilizing the Isofit® Software developed by Aksenenko and Miller (Möbius, Miller, & Fainerman, 2001). As noted previously for other whey protein systems, the adsorption of protein is different compared to other typical

surfactants, due to structural reorganization and electrostatic or hydrophobic interactions between adsorbed molecules at the interface (Pradines, Krägel, Fainerman, & Miller, 2008). In this system, the Langmuir model best fit the protein-only system, while the Frumkin model was employed on the phytosterol-system. The following equations (2-7) describe the isotherm models employed (Möbius et al., 2001).

$$-\frac{\Pi\omega}{RT} = \ln(1 - \Gamma\omega) + \alpha(\Gamma\omega)^2 \quad (2)$$

where $\Pi = \gamma_{lvo} - \gamma_{lv}$ is the surface pressure, ω is the molar area, Γ is the surface excess and α is the interaction parameter between adsorbed adjacent surfactant molecules at the oil-water interface. The adsorption isotherm for Frumkin model is given by:

$$bc = \frac{\Gamma\omega}{1-\Gamma\omega} \exp(-2\alpha\Gamma\omega) \quad (3)$$

where b is the adsorption rate constant and c is the bulk concentration of surfactant. With surface coverage given by $\theta = \Gamma\omega$, equations 1 and 2 can be written as:

$$-\frac{\Pi\omega}{RT} = \ln(1 - \theta) + \alpha(\theta)^2 \quad (4)$$

$$bc = \frac{\theta}{1-\theta} \exp(-2\alpha\theta) \quad (5)$$

There are three model parameters, b , ω and α . When $\alpha=0$, i.e. when there is no interaction between adsorbed surfactant molecules, the Frumkin equation limits to a Langmuir isotherm.

$$-\frac{\Pi\omega}{RT} = \ln(1 - \theta) \quad (6)$$

$$bc = \frac{\theta}{1-\theta} \quad (7)$$

These models were used to calculate the interfacial concentration of phytosterol and whey protein at different concentrations necessary for the employment of regular solution theory, which will be described in detail in the upcoming sections.

2.5 Statistical Analysis

Mean values \pm standard deviations of the data were reported for each emulsion formulation. Results were analysed for statistical significance utilizing SAS® 9.3 software for Windows. A *Tukey's Post Hoc* Difference Test with a level of probability at $p < 0.05$ was used to analyze significant differences between treatments.

3. Results

3.1 Shape, Size, and Morphology

3.1.1 Particle Size

The particle size of emulsions enriched with 0.0% (control), 0.3%, and 0.6%, wt/wt of phytosterol were expressed as the mean of volume-weighted distributions ($D_{(4,3)}$). Phytosterol addition resulted in a significant decrease ($p < 0.05$) in $D_{(4,3)}$ values of all emulsions, from $0.85 \pm 0.02 \mu\text{m}$ in the control emulsion to $0.78 \pm 0.03 \mu\text{m}$ or $0.70 \pm 0.01 \mu\text{m}$ in the 0.3% and 0.6% PE emulsions, respectively. Decreases in particle size have been observed previously with phytosterol enrichment in milk fat-based emulsions (Zychowski et al., 2016). Statistically significant decreases in particle size have been observed previously with phytosterol enrichment in milk fat-based emulsions (Zychowski et al., 2018; Zychowski et al., 2016). The overall droplet size distribution ranged from 0.1 to $16.4 \mu\text{m}$ (Fig. 1). The decrease in $D_{(4,3)}$ from PE was observed by a slight increase in smaller droplet sized peak, which was observed in the collected microscopy data and is detailed further below.

3.1.2 Polarized Light Microscopy

Figure 2 shows polarized light microscopy (PLM) images of the 0.6% PE emulsion with milk fat as the carrier matrix at 20°C and 50°C . Crystalline material can be identified by its optical response to polarization through light birefringence and is commonly used to

establish the presence of crystalline material within food matrices (Chen, Guo, Wang, Yin, & Yang, 2016; Maher, Auty, Roos, Zychowski, & Fenelon, 2015; Thivilliers, Laurichesse, Saadaoui, Leal-Calderon, & Schmitt, 2008; Toro- Vazquez, Rangel- Vargas, Dibildox- Alvarado, & Charó- Alonso, 2005). Birefringence within the 0.6% PE emulsion appeared at both temperatures, which confirmed the presence of phytosterol derived crystalline material, as 50 °C is above the melting point of AMF but below that of phytosterols within a TAG matrix (Acevedo & Franchetti, 2016; Lopez et al., 2007). Birefringence within the 0.0% and 0.3% PE emulsion was not seen in emulsion droplets and is discussed in more detail below (data not shown).

3.1.3 Confocal Laser Scanning Microscopy.

Confocal laser scanning microscopy (CSLM) with fluorescent staining was performed to examine the lipid and protein distribution within PE emulsions (Fig. 3). Images were captured at 3 and 5x magnification with protein and lipid components labelled as red and green, respectively. Protein and lipid fluorescent channels were overlapped in all CLSM images, except the zoomed in protein image for the 0.6% PE emulsion at 5x magnification. Images were found to agree with the given particle size distribution and in general, smaller droplets were found in images in with higher level of plant sterols as observed previously (Fig. 1 ; Zychowski et al., 2016).

No morphological differences were observed between the control and 0.3% PE emulsion. Conversely, in the 0.6% PE emulsion, detectable crystals, identified by negative contrast as straight edges, were present within and at the surface of larger emulsion droplets, as observed previously (Zychowski et al., 2016). Separated protein scans of the 0.6% PE emulsion demonstrated how crystalline material is distributed within the emulsion and appears to disrupt protein coverage on the lipid droplets.

3.1.4 Cryo-scanning Electron Microscopy

Droplet surface and fracture morphology was visualized utilizing cryo-scanning electron microscopy (Cryo-SEM; Fig. 4). Cryogenic fracturing enabled the visualization of cross-sections of the emulsion samples. The control emulsion contained relatively smooth droplets, as seen in the confocal images (Fig. 3). The 0.3% and 0.6% PE emulsions both contained droplet cross-sections showing straight-edged and angular/needle-like structures within the emulsions droplets, consistent with PLM micrographs (Fig. 2) and other cryo-images of fat crystals (Heertje, 1993). Besides having droplets containing crystalline material, the 0.6% PE emulsion sample had some larger **coalesced** droplets, which had altered and roughened surfaces, suggestive of crystalline material at the droplet interface (Rousseau, 2000). A similar surface morphology has been observed in other food systems, such as margarine or cocoa butter emulsions, which exploit surface crystals to stabilize the interface (Heertje, 1993; Norton & Fryer, 2012).

3.2 Interfacial Tension and Modeling of Emulsion Systems

3.2.1 Interfacial Tension

Interfacial tension was measured at 60 °C to understand the interactions of phytosterols and whey protein at the interface during initial emulsion formation and homogenization (Table 1; Fig. 5a & b). In agreement with previous research, the initial interfacial tension (γ_I 0 min) of water with medium-chain triglyceride (MCT) oil (water/MCT), was found to be 20.4 ± 0.5 mN/m (Jumaa & Müller, 1998; Mao et al., 2009). Upon the addition of just 2% phytosterol (0.2% wt/wt if emulsified), to the oil phase, there is a significant decrease in observed initial γ_I , as compared to the water/MCT sample. Correspondingly, every 1% increase in phytosterol, with a water-only aqueous phase, resulted in a further significant decrease in initial γ_I . The water/6% phytosterol sample, had a value of 9.3 ± 0.3 mN/m, which was the lowest of all of

the water/phytosterol interfaces and was similar to that of the 1% protein/MCT sample with an initial γ_I value of 10.0 ± 0.4 mN/m (Table 1). The water/6% phytosterol sample also had a slight increase in interfacial tension values at 5 and 30 min but, since these values all fall within the standard deviation, this was not deemed significant.

When phytosterol and protein addition were added separately, both decreased initial interface tension, but interfaces with $\geq 3\%$ phytosterol and whey protein combined had a significantly lower initial γ_I ($p < 0.05$) than all other samples. The lowest initial γ_I was of the 1% protein/5% phytosterol and 1% protein/6% phytosterol interfaces, at 3.6 ± 0.5 mN/m and 2.7 ± 0.5 mN/m, respectively (Table 1). These results for initial γ_I describe the ability of both phytosterols and whey protein to move to the interface and influence the interfacial tension at an oil/water surface both separately and synergistically. Both phytosterols and whey protein possess an amphiphilic molecular structure and their ability to influence interfacial tension separately is expected (Chen et al., 2016; McClements, 2004; Rossi, ten Hoorn, Melnikov, & Velikov, 2010; Rouimi, Schorsch, Valentini, & Vaslin, 2005). However, a synergistic effect between these two molecules has not been recorded previously and will be further discussed later.

The interfaces were continuously monitored for 5 min, then in subsequent 5 min intervals for 30 mins. Final values at 5 min (γ_I 5 min) and 30 min (γ_I 30 min) were compared against the initial γ_I (Δ 0-5 min and Δ 0-30 min, respectively), as a quantitative means of evaluation (Table 1; Fig. 5a & b). By comparing changes within these two time points, several features regarding interface formation can be described. Firstly, 1% phytosterols and whey protein separated at the interface had statistically similar Δ 0-5 min values, but the 1% whey protein sample had a larger Δ 0-30 min value (Table 1). This demonstrated that whey protein can decrease interfacial tension more than phytosterols, but during initial emulsion formation

their ability is relatively similar. Secondly, the largest initial change in interfacial tension occurred for the 1% protein/4% phytosterol sample but, at 30 min, the overall change in tension was similar to other samples (Table 1; Fig. 5b). Thus, this multicomponent interface demonstrates that this synergistic interfacial effect acts quickly upon the oil/water interface.

3.2.2 Interfacial Modeling

The ability of surfactants to synergistically influence interfacial tensions has been previously studied by several authors (Zhou & Rosen, 2003)(Reddy & Ghosh, 2010; Rosen & Hua, 1982; Rosen & Zhou, 2001). To model this relationship, final interfacial tension results were graphed on wt/wt % of each component and the mixed phytosterol and whey protein interfaces (Fig. 6). A synergic relationship between whey protein and phytosterols was apparent, as phytosterol concentrations higher than 3% at 1% protein had a lower final γ_I values than the two components separately. This data was then processed by the regular solution theory (RST) developed by Rubingh and altered by Rosen and Hau (1982) to account for the possible interaction between phytosterols and whey protein at the surface of an oil and water system (Rosen & Hua, 1982; Rubingh, 1979). The approach by Rosen and Hua takes the non-ideality of mixing two compounds into consideration through a molecular interaction parameter, β (eq. 8) (Rosen & Hua, 1982). The magnitude of the interaction parameter corresponds to the deviation from ideal solution behavior. Negative values of the interaction parameter signify that the attractive interaction between the surfactants in the mixture is greater than the self-attraction of each surfactant. Positive values indicate repulsive interactions between the surfactants. The molecular interaction parameter, β , is defined by equation 8.

$$\beta = \frac{\ln\left(\frac{C_s}{x_s C_s^o}\right)}{(1-x_s)^2} \quad (8)$$

where, C_s is the bulk concentration of surfactant (phytosterols) in the mixture, x_s is the interfacial composition of surfactant, and C_s^o is the bulk concentration of pure surfactant required to achieve the same interfacial tension of the mixture.

Rosen and Hua showed that the interfacial composition (x_s) can be calculated by utilizing equation 9 (Rosen & Hua, 1982). Here, C_s and x_s refer to the phytosterols concentrations, while C_p and x_p correspond to the protein bulk concentration and interfacial composition, respectively.

$$\frac{x_s^2 \ln\left(\frac{C_s}{x_s C_s^o}\right)}{(1-x_s)^2 \ln\left(\frac{C_p}{(1-x_s) C_p^o}\right)} = 1 \quad (9)$$

To solve for x_s , C_s^o and C_p^o are needed, which are the bulk concentrations of pure surfactants (phytosterols and WPI) required to achieve the same interfacial tension as that of the mixture. Values for C_s^o and C_p^o were derived from the adsorption isotherm, Langmuir and Frumkin for whey protein and phytosterol, respectively (Eq. 9 & Fig. 7).

For a fixed bulk protein concentration of 1 wt%, with increasing phytosterol concentration, the interaction parameter and the interfacial composition were calculated to better understand the synergistic effect of protein and phytosterols at the interface (eq. 8-9; Table 2). The interaction parameter was negative, suggesting attractive behavior between the adsorbed proteins and phytosterols at the interface (Rosen & Hua, 1982; Zhou & Rosen, 2003). However, after the interfacial tension of the systems reaches its lower limit at 4% sterol and 1% protein, the interaction parameter remains relatively constant, even decreasing slightly upon phytosterol addition (Table 2).

As seen previously within other whey protein-surfactant complexes (β -lactoglobulin with sodium dodecyl sulfate or cetyltrimethylammonium bromide), once the interface is

saturated with the complex, additional surfactant can lead to less surface-active complexes, which then have to compete with free surfactant molecules (Wüstneck, Krägel, Miller, Wilde, & Clark, 1996). Subsequently, as the concentration of phytosterol in the lipid phase increased from 2-6 wt%, the calculated interfacial composition of phytosterols increased from 54 to 88 mol% (Table 2). This indicates that, during emulsion formation, phytosterols can outcompete whey protein/whey protein complexes for space at the oil/water interface. Preliminary results showed that it was not possible to form emulsions consisting of $\geq 8\%$ phytosterol and 1% protein or phytosterols alone; this confirms that, at higher levels of phytosterol addition, the interfacial composition is indeed different and dominated by phytosterols (Zychowski et al., 2016).

Even though the RST approach is strictly only valid when both the surfactants are present in a single phase, it is surprising that the theory gives a qualitative picture of the interfacial composition when the surfactants adsorb from two different phases, which is the case for proteins and phytosterols that are dispersed within the oil and aqueous phase, respectively. The calculations presented in this section are intended for a qualitative explanation of synergistic behavior of phytosterols and proteins at the oil/water interface.

4. Discussion

4.1 Influence of Phytosterol Addition on the Morphology and Physical Properties of Emulsions.

Particle size and images captured using PLM, CSLM, and cryo-SEM demonstrated the effect of phytosterol enrichment on the emulsion system. Particle size of the PE emulsion significantly decreased with each subsequent addition of phytosterols into the oil phase between separate emulsion trials. Although the trend was similar, the extent of difference

between trials was less than what was observed previously using a different homogenizer and mastersizer (Zychowski et al., 2016). A decrease in emulsion droplet size was also recorded in a study which analyzed the stability of oil-in-water loaded MgCl_2 emulsions with phytosterols enriched into the continuous phase. Emulsion droplets dispersed with the phytosterol containing lipid were found to be smaller upon initial formation and were able to resist coalescence unlike the control sample without phytosterols. In the same study, this was further investigated by studying the o/w interface with and without the presence of phytosterols and results demonstrated that the presence of phytosterols significantly influenced the adsorption behaviour of the both of the emulsifiers used, polyglycerol polyricinoleate (PGPR) and sodium caseinate (Andrade & Corredig, 2016). Phytosterols have also been documented to decrease interfacial tension without the presence of protein, as observed within the current and previous studies (Table 1 & Fig. 5b; Cercaci, et al., 2007). Thus, it is hypothesised that the recorded decrease in particle size could be due to the presence of phytosterols at the oil-in-water interface.

However, it should be noted that this change in particle size was not significant enough to change the stability of these PE emulsions over time. In a follow up study performed by this group, PE emulsions were evaluated for emulsion instability over 1 month with a similar particle size and trend as recorded within this study; sizes were control= 0.94 ± 0.06 , 0.3%= 0.86 ± 0.06 , 0.06%= 0.73 ± 0.07 μm . In addition, PE emulsions were created at 0.2 μm for comparison via high pressure homogenisation. In this study, no significant change in stability ($p < 0.05$) was observed in the emulsions created with or without phytosterols after 1 week or 1 month of formation that possessed had a particle size of 0.94-0.73 μm . The PE emulsion with an average droplet size of 0.2 μm were found to be significantly more stable overtime than the PE emulsions with the larger particle size, indicating the need for large differences in average

droplet sizes to observe significant differences in stability (Zychowski et al., 2018). Interestingly, no significant difference was observed in stability upon the addition of phytosterols into the emulsion systems; typically, the presence of crystals within an emulsion system causes emulsion destabilisation, by means particle coalescence of the lipid droplets (McClements, 2012). However, destabilisation due to the presence phytosterol crystals was not observed within this system, nor in other emulsion systems containing phytosterols (Andrade & Corredig, 2016; Chen et al., 2016). This is most likely due to ability of phytosterols to form a stable contact angle at the oil and water interface, which is discussed in more detail below.

PLM images were captured at 20°C and 50°C, as AMF melts completely at ~40°C and phytosterol within TAG systems at around ~60°C (Fig. 2; Acevedo et al., 2016; Lopez et al., 2007; Zychowski et al., 2016). Birefringence in the images was used to distinguish the presence of crystalline material within the emulsion systems. Thus, the birefringence observed at 50 °C, above the melting point of AMF, confirms that the observed crystals in images are indeed composed of phytosterols. No crystalline AMF was observed in the 0.0% and 0.3% samples, despite the sample being held at 20°C for 24 h.

This was most likely due to the size of the milk crystals produced during this time being insufficient to be detected by the polarised light microscope. Similarly, Truong et al. (2014) captured images of milk fat-based emulsions after aging at 4 °C for 24 using cryogenic transmission electron microscopy (cryo-TEM). In the images of milk fat-based emulsion ranging from 0.73 to 0.23 µm in size, no large crystals were apparent at the interface or in the captured cross sections of the emulsion droplets; only a fine crystalline network was made visible through the use of high powered Cryo-TEM. Similar results have been observed in lard-based emulsions, where fine crystals could not be observed *via* polarised light and larger

protruding lard crystals could only be observed in some emulsion droplets after holding for several hours (S. D. Campbell, Goff, & Rousseau, 2001)

Images captured using CSLM differentiated between the lipid and protein components of the PE emulsions. Previous CSLM images published by Zychowski et al. (2016) showed an altered interface present within 0.6% PE emulsion, as seen in this study, but did not clearly capture the protein layer distribution around fat droplets. In Figure 3, all PE emulsions can be visualized, along with the images taken from the separated protein and lipid channels for the 0.6% PE emulsion. The separated channel images show protein coverage around the lipid droplet of the 0.6% PE emulsion, except where phytosterol interfacial crystals were present (Fig. 3; Image 3b). This gap in protein coverage supports the hypothesis of phytosterols being present at the interface and suggests that possibility that phytosterols can stabilize the interface of an emulsion droplet. Phytosterol stabilization at the interface was also observed in PE sunflower oil emulsions with octenyl succinic anhydride starch as the main emulsifier. Phytosterols were able to co-crystallize with the starch and this complex formed a strong barrier around the dispersed oil droplets. After 90 d emulsions containing phytosterols were ~8 times smaller than the control emulsion with starch alone, which had **coalesced**, demonstrating the ability of crystalline phytosterols to successfully stabilize an interface (Chen et al., 2016).

Cross-sectional images taken using cryo-SEM highlight how phytosterol crystallization influences the surface morphology of emulsion droplets (Fig. 4). Micrographs of the control and 0.3% PE emulsions show droplets with a relatively smooth surface, compared to the **coalesced** droplets present in the 0.6% PE emulsion. These larger droplets facilitate the visualization of the presence of phytosterol crystals but, in line with previous studies, did not result in significant destabilization of the PE emulsion system (Zychowski et al., 2016).

Crystallization within emulsions usually results in partial **coalescence**, which leads to particle aggregation and eventual emulsion destabilization (McClements, 2012). As mentioned, phytosterols have been previously documented to crystallize at the interface but not destabilize the emulsion. Although phytosterol crystallization might not result in emulsion destabilization, it can decrease bioaccessibility within the functional food systems (Jones & AbuMweis, 2009). For example, in a study performed by Nestec, 1.8 g of non-esterified phytosterols were solubilised in a milk matrix and consumed; the solubilised phytosterol ester resulted in a $29.1 \pm 4.1\%$ reduction in LDL-cholesterol levels (Pouteau et al., 2003). Conversely, 3 g of crystallised phytosterols administered in a crystallised tablet were only able to decrease LDL-cholesterol levels by 11.0% (Carr, Krogstrand, Schlegel, & Fernandez, 2009). In a side by side study, 0.7 g solubilised phytosterols in micelles were ~25% more effective in reducing LDL cholesterol level than 1 g of powdered crystalline phytosterols (Ostlund, Spilburg, & Stenson, 1999). The discrepancy between these results highlights the need for further research on factors that influence phytosterol solubility in food matrices.

4.2 The Influence of Phytosterols and Whey protein on Interfacial Tension.

Dynamic γ_I values were evaluated under several different concentrations of phytosterols and whey protein to understand the influence of each component individually and with various combinations of emulsion formations (Table 1; Fig. 5a & b). The unadulterated surface for all measurements is the initial γ_I of the interface with MCT oil and water, as adjustments to this interface resulted from the addition of either phytosterol to the oil phase and/or whey protein isolate to the water phase (Drapala et al., 2015). When $\geq 2\%$ phytosterols were added to the oil phase, initial γ_I values decreased significantly ($p < 0.05$; Table 1). The ability of phytosterols to decrease γ_I has been observed previously in an experiment employing hexane, as the lipid phase, with dissolved phytosterols; results demonstrated that even low

phytosterol concentrations (1 mmol/kg) in hexadecane were able to significantly decrease γ_I , while higher phytosterol concentrations could further decrease γ_I (Cercaci et al., 2007). Phytosterols such as β -sitosterol, campesterol and stigmasterol possess a hydrophobic, tetracyclic, fused-ring skeleton and a polar, hydroxyl group. The differing polarities within their chemical structure give phytosterols a slightly amphiphilic nature, allowing them to interact with both the aqueous and lipid phases at oil-water interfaces (Chen et al., 2016; Rossi et al., 2010).

As expected, whey protein, consisting mainly of β -lactoglobulin, was also able to decrease interfacial tension in the absence of phytosterols (Table 1 & Fig. 5a). Even with the addition of only 0.5% whey protein, the initial γ_I significantly decreased but, unlike phytosterol addition, increasing the concentration of protein (0.5-3%) had little effect on γ_I values (Table 1). It is hypothesized that whey protein at 0.5% had already saturated the MCT and water interface, and thus increasing protein concentration was not able to significantly further decrease interfacial tension (Dickinson, 1999; McClements, 2004). Whey proteins are comprised of large globular proteins, and the rate at which they adsorb at the oil-water interface is limited by their size, compared to other smaller surfactants; however, they have been shown to provide long-term stability to oil-water interfaces (Courthaudon, Dickinson, Matsumura, & Williams, 1991; McClements, 2015). Thus, it not surprising that whey proteins were able to significantly reduce initial γ_I and over time had a much larger $\Delta(\gamma_I \text{ init} - \gamma_I \text{ 30 min})$, as compared to the phytosterol/water interfaces. Similar interfacial results for whey protein and oil interfaces have been observed previously (Drapala et al., 2015; Li, Auty, O'Mahony, Kelly, & Brodkorb, 2016; Sünder, Scherze, & Muschiolik, 2001).

Most interestingly, the lowest initial γ_I values came from interfaces containing 3% \geq phytosterols and whey protein (Table 1) but, as can be noted, all levels of phytosterol

concentration influenced interfacial tension in the presence of protein (Fig. 5b). In addition, the largest (Δ 0-5 min) value was achieved with the 1.0% protein/4.0% phytosterol interface at 3.2 ± 0.6 mN/m (Table 1). This data suggests that phytosterols and whey protein synergistically reduce interfacial tension and are able to interact at the interface more quickly together than when separated. Thus, the authors believe that whey proteins and phytosterols can be considered to participate in synergism at the emulsion interface. Synergism is defined here as “the condition in which the properties of the surfactant mixture are better than those attainable with the individual surfactants by themselves” (Reddy & Ghosh, 2010).

The interaction between phytosterols and whey protein was quantified using RST modified by Rosen and Hua (Rosen & Hua, 1982; Rubingh, 1979). In mixed interfaces with 1% protein and 1-6% phytosterol, the interaction parameter was found to be negative, suggesting that phytosterols and whey protein are interacting at the surface interface (Zhou & Rosen, 2003). Within the bulk system, both the whey protein and phytosterols have negative electric-static charges (Rossi et al., 2010; Zychowski et al., 2016); however, phytosterols possess a negatively charged hydroxyl group, which most likely interacts at the interface, while the remaining portions of the molecule are relatively neutral.

Although there are limited studies investigating the binding properties of phytosterols and proteins, a patent by Monstanto has previously described the technology of using egg proteins to limit the crystallization behaviour of phytosterols, as the two compounds are believed to form a complex. The patent technology entails heating an edible food-grade triglyceride-based system to 60 °C in order to melt the phytosterols. Egg protein, dissolved in water, is then added with lecithin and an emulsion is created. The mixture is then dried, and it is believed that phytosterol crystallisation was limited by the egg protein addition (Corliss, Finley, Basu, Kincs, & Howard, 2000).

In a follow up study by the Zychowski et al. (2018), emulsions with lecithin and whey protein were found, using synchrotron X-ray scattering, to prevent phytosterol crystallisation to a greater degree than phytosterol and whey protein emulsions without lecithin alone. Lecithin, consisting mostly of phospholipids, is well known for its ability to solubilize phytosterols within micelles and can prevent phytosterol crystallisation (Ostlund et al., 1999). Thus in the described Monsanto patents, it is unclear if the decrease in phytosterol crystallisation is due to the presence of egg protein and/or addition of lecithin into the emulsion-based systems. Phytosterols have also been documented via fluorescence probes to bind with the fungal protein called elicithin. This cysteine rich-protein functions as an extracellular sterol carrier protein and provides the fungi with phytosterols which are needed for plant membrane synthesis, as some *Phytophthora* fungi cannot synthesize phytosterols internally (Mikes et al., 1998). Whey proteins also possess a high concentration of cysteine amino acids, which could also aid in its ability to interact with phytosterols at the emulsion interface (Keri Marshall, 2004).

The interaction parameter reached its most negative result (strongest interaction) at 4% phytosterol and 1% protein, which also coincided with the lower limit of interfacial tension on the tensiometer. Phytosterol levels $\geq 5\%$ resulted in lower levels of protein adsorption and higher levels of phytosterol adsorption and interaction parameters. In other whey protein-surfactant systems, once protein adsorption has been saturated, additional surfactant has been found to drive hydrophobic interaction between the complexes. This leads to decreased surface activity of the complex and, thus, the complex must compete for the interface with free surfactant molecules (Wüstneck et al., 1996). Results from the previously conducted study by Zychowski et al. (2016), found that in emulsions with $\geq 8\%$ phytosterols and 1% protein or phytosterols alone were not stable and could not be homogenized. This confirms the calculated

results, suggesting that, at a higher concentration of phytosterol enrichment, the interfacial composition is dominated by phytosterols. The results calculated *via* RST serve as quantification of the interaction between phytosterols and whey proteins at the surface interface.

This synergism was recorded and modelled to occur at the interface at 60 °C, which was the temperature at which the emulsions were formed, indicating potential relationship between phytosterols and whey proteins at this temperature. However, these emulsions were cooled to 20 °C for storage and, during this time, the phytosterols were found to crystallize in both the 0.3% and 0.6% emulsion (Zychowski et al., 2018). At 20 °C in the 0.6% PE emulsion some of the phytosterol crystalline material appears to be present at the interface, as changes in morphology are visible from microscopy images (Fig. 2 -4). Thus, it is hypothesised that phytosterols and proteins remain at the interface and within the droplet during this cooling process and impact the morphology and the size of the emulsion droplets. However, it is important to consider how the interfacial tension could be changing during this cooling process and how phytosterol crystallization at the o/w interface could be influencing this process.

Regarding interfacial tension research has demonstrated that as the temperature of an o/w system containing a surfactant decreases, so does the interfacial tension (Salager, Morgan, Schechter, Wade, & Vasquez, 1979; Spaepen, 1994). As this system cools further, the free energy of the system increases until the activation energy for crystallisation is reached. Once this activation energy is met, nuclei form and a negative change in free energy occurs (Damodaran, Parkin, & Fennema, 2007; Widlak, Hartel, & Narine, 2001). These nuclei grow into crystals which can stabilise or destabilise an interface based on the wetting properties of the solid-crystal at the oil and water interface. If the crystal forms a contact angle between the

oil and water interface of less than 90° , the crystal can stabilise an o/w emulsion (Rousseau, 2000).

In non-food system, colloidal particles such as paraffin wax can be used to stabilise an emulsion system without the use of an emulsifier. In food systems generally, the presence of some surfactant is required. The properties of these surfactants can change the observed contact angle and, thus, the observed interfacial tension (Rousseau, 2000). Campbell (1989) evaluated palm oil fat crystals for contact angle at the o/w interface and emulsion stability using different emulsifiers (3 different monoacylglycerols (MAG), Span 80, lecithin and sodium caseinate). Interestingly MAG, Span 80 and lecithin had no effect on the contact angle of the palm oil crystals. However after 1% sodium caseinate was added into the solution, smaller contact angles were observed with concurrently more stable emulsions. This was believed to be due to the protein being able to alter the polar interactions between the emulsifiers and crystals, which ultimately led to a decrease in the contact angles.

In a similar study, glycerol monopalmitate (GMP), a fat which crystallises around 18°C , was added to an oil and water interface and the system was crystallised between 40°C to 1°C . As the interface with only GMP, oil and water cooled, crystallisation was observed as a sharp decline in interfacial tension. Conversely, milk proteins alone were added into the aqueous phase and interfacial tension was found not to change significantly across the temperature range. However, when GMP and milk protein were combined, the two gave a lower interfacial tension than what was observed separately. During GMP crystallisation the combined interface decreased significantly, as observed during GMS crystallisation alone but the GMP appeared to “squeezed out” the milk proteins presence at the interface (Krog & Larsson, 1992).

In our system, at room temperature, it can be judged that the PE emulsion interface is not completely covered in phytosterol crystals even at 0.6% PE, and that protein is present at the interface (Fig. 3). Confocal images detail the displacement of protein from the oil and water interface where phytosterols crystals are present, as reported by Krog & Larsson (1992). However, during emulsion formation, it is believed that both phytosterols and whey protein interact synergistically, as modelled and observed with interfacial tension measurement; this interaction gives rises to significantly smaller emulsion droplets and the observed changes in emulsion morphology. During cooling, the interfacial tension most likely decreases and some of the phytosterol present at the interface crystallise. The extent of the interaction between whey protein and phytosterols has yet to be studied at lower temperatures, along with the actual contact angle of phytosterols at o/w interfaces and this could examined in future studies. However, despite the presence of phytosterol crystals, PE enriched emulsion, up to 0.6% wt/wt, remain stable over the course of a month, as compared to emulsions without phytosterols present, suggesting that these phytosterols do not destabilise the interface significantly.

5. Conclusions

Phytosterol crystallization impacts the bioaccessibility of bioactive compounds and can possibly occur at the interface phytosterol-enriched emulsion as demonstrated by confocal, cryo-SEM, and polarized light microscopy. Upon examining the emulsion interface, interfacial tension results demonstrated that both phytosterols and whey proteins were able to lower interfacial tension. However, the combination of phytosterols and whey protein was able to lower interfacial tension to a greater extent than the two components separately, demonstrating synergism between the two compounds. These results were confirmed by interfacial modeling results, suggesting that the two compounds were interacting at the interface. This type of behavior between phytosterols and whey protein is not well studied and highlights a novel

exploitable characteristic of phytosterols, which can be utilized within the functional food industry. Additionally, this work highlights the need to monitor crystallization within and at the surface of the phytosterol-enriched matrices to improve bioaccessibility in the final food product.

6. Acknowledgements

The authors would like to thank the Teagasc Food Research Centre for its support (Teagasc Project RMIS6412) and assistance in organizing this collaborative project with Melbourne University. The authors would also like to thank Kamil Drapala for his guidance and help utilizing the Kruss Tensiometer at the University College of Cork and Li Day at AgResearch for her assistance. Finally, the authors would like to thank Lisa Blazo from the University of Sheffield for her assistance in editing the manuscript.

Tables

Table 1 Interfacial tension for oil and water systems containing different concentrations of whey protein and phytosterols. All interfaces contained water and medium chain triglycerides, but some interfaces were respectively enriched with either/both whey protein and phytosterols.

Interface	Interfacial tension (γ_I) (mN/m)				
	0 min	5 min	30 min	Δ (0-5 min)	Δ (0-30min)
Water/mct	20.4 \pm 0.5 ^a	19.9 \pm 0.4 ^a	19.6 \pm 0.3 ^a	0.5 \pm 0.6 ^{abcd}	0.9 \pm 0.6 ^{abc}
Water/1% ps	20.3 \pm 0.2 ^a	19.5 \pm 0.2 ^a	18.6 \pm 0.5 ^a	0.8 \pm 0.3 ^{abe}	1.7 \pm 0.6 ^{bc}
Water/2% ps	17.4 \pm 0.4 ^b	17.2 \pm 0.5 ^b	16.6 \pm 0.6 ^b	0.2 \pm 0.6 ^{abcdf}	0.8 \pm 0.7 ^{abc}
Water/3% ps	15.6 \pm 0.1 ^c	15.6 \pm 0.1 ^c	15.5 \pm 0.2 ^b	0.1 \pm 0.2 ^{bcd}	0.1 \pm 0.2 ^{de}
Water/4% ps	13.6 \pm 0.4 ^d	13.6 \pm 0.4 ^d	13.6 \pm 0.4 ^c	0.0 \pm 0.6 ^{df}	0.0 \pm 0.7 ^{de}
Water/5% ps	11.2 \pm 0.5 ^e	11.2 \pm 0.5 ^e	10.8 \pm 0.5 ^d	0.0 \pm 0.8 ^{cdf}	0.4 \pm 0.7 ^{ad}
Water/6% ps	9.3 \pm 0.3 ^f	9.6 \pm 0.3 ^f	10.2 \pm 0.7 ^d	-0.3 \pm 0.4 ^f	-0.9 \pm 0.7 ^e
0.5% pro/mct	10.0 \pm 0.5 ^{ef}	9.3 \pm 0.6 ^{gf}	6.8 \pm 0.4 ^e	0.8 \pm 0.8 ^{abce}	3.3 \pm 0.7 ^{fg}
1.0% pro/mct	10.0 \pm 0.4 ^{ef}	9.1 \pm 0.3 ^{gf}	6.3 \pm 0.3 ^{ef}	0.9 \pm 0.5 ^{ace}	3.7 \pm 0.5 ^{gh}
1.5% pro/mct	9.2 \pm 0.5 ^f	8.7 \pm 0.4 ^{gf}	6.2 \pm 0.5 ^{ef}	0.6 \pm 0.6 ^{abcd}	3.0 \pm 0.7 ^{fg}
2.0% pro/mct	9.7 \pm 0.4 ^f	8.2 \pm 0.3 ^{gh}	5.8 \pm 0.1 ^{efg}	1.5 \pm 0.5 ^{ghe}	3.9 \pm 0.4 ^{gh}
3.0% pro/mct	9.6 \pm 0.6 ^f	8.3 \pm 0.5 ^{gh}	5.9 \pm 0.7 ^{efg}	1.3 \pm 0.8 ^{egh}	3.8 \pm 0.9 ^{gh}
1.0% pro/1.0% ps	9.1 \pm 0.2 ^f	8.3 \pm 0.1 ^{gh}	6.9 \pm 0.2 ^e	0.8 \pm 0.2 ^{abe}	2.2 \pm 0.2 ^{cf}
1.0% pro/2.0% ps	9.4 \pm 0.2 ^f	7.5 \pm 0.1 ^h	5.4 \pm 0.1 ^{fg}	1.9 \pm 0.2 ^h	4.1 \pm 0.2 ^{ghi}
1.0% pro/3.0% ps	7.3 \pm 0.5 ^g	5.8 \pm 0.3 ⁱ	3.5 \pm 0.2 ^{hi}	1.5 \pm 0.6 ^{egh}	3.8 \pm 0.6 ^{gh}
1.0% pro/4.0% ps	5.9 \pm 0.6 ^h	2.7 \pm 0.2 ^j	2.2 \pm 0.4 ^j	3.2 \pm 0.6 ⁱ	3.6 \pm 0.7 ^{gh}
1.0% pro/5.0% ps	3.6 \pm 0.5 ⁱ	2.7 \pm 0.1 ^j	2.3 \pm 0.3 ^j	0.9 \pm 0.5 ^{ace}	1.3 \pm 0.6 ^{abc}
1.0% pro/6.0% ps	2.7 \pm 0.5 ⁱ	2.5 \pm 0.5 ^j	2.6 \pm 0.3 ^{ij}	0.2 \pm 0.7 ^{abcd}	0.1 \pm 0.6 ^{de}

Within a column, values with different superscript letters are significantly different ($p < 0.05$).

Δ =Difference between γ_I values at different time points.

Table 2: Interfacial composition of phytosterols and protein as a function of phytosterol concentration in bulk oil phase

Bulk Total Concentration (wt%)	Bulk Phytosterols Concentration W_s (wt%)	Bulk Protein Concentration W_p (wt%)	Interfacial Tension (mN/m)	Interfacial composition phytosterols x_s (mol%)	Interfacial Composition Protein x_p (mol%)	Interaction parameter (β)
3	2	1	5.4	54	46	-2.90
4	3	1	3.5	69	31	-5.05
5	4	1	2.2	77	23	-6.74
6	5	1	2.3	82	18	-5.64
7	6	1	2.6	88	12	-4.42

The interface with 1% phytosterol and 1% bulk protein was not included as it did not converge with the Rosen and Hau model (Rosen & Hua, 1982). Interfacial tension measurements were taken after 30 min at 60°C.

Figure Captions.

Figure 1. Particle size distribution of emulsions with 10% milk fat: 1% protein: 89% H₂O with different phytosterol-enrichment (PE) levels: (Δ) 0.0% PE emulsion (the control), (\blacksquare) 0.3% PE emulsion, (\bullet) 0.6% PE emulsion.

Figure 2. Polarized light micrograph (partially uncrossed polar filters) of 0.6% w/w phytosterol emulsion showing elongated birefringent crystals associated with fat droplets (arrows) at 20°C and 50°C. Scale bar = 10 μ m. PC = phytosterol crystal.

Figure 3. Confocal laser scanning images of phytosterol-enriched (PE) emulsions at 3 and 5x magnification, superscripted as 'a' and 'b', respectively. Emulsions are labelled as (1) 0.0% PE emulsion (control), (2) 0.3% PE emulsion, and (3) 0.6% PE emulsion. Images show the distribution of fat and protein, with fat represented in green and protein in red. Image 3b shows an enlarged section of a protein only-scan of PE emulsion droplets with phytosterol crystals. Scale bar = 10 μ m. Note: crystalline phytosterols both at the interface and within fat droplets are made visible by negative contrast (white arrows). PC = phytosterol crystal.

Figure 4. Cryo-scanning electron micrographs of cross sections of emulsions with different levels of phytosterol enrichment. Emulsions are labelled as (1) 0.0% PE emulsion (control), (2) 0.3% PE emulsion and (3) 0.6% PE emulsion. Enlarged section highlights the presence of crystal-like material inside of emulsion droplets. Scale bar = 10 μ m.

Figure 5. (a) Dynamic interfacial tension measurements of samples over 30 min at 60 °C. All interfaces contained water (aqueous phase) and MCT (oil) but some phases were enriched with either whey protein and/or phytosterol, respectively. Interfaces are denoted as (▲) water/MCT, (●) water/3% phytosterol, (■) water/6% phytosterol, (▲) 1% protein/MCT, (■) 1% protein/3% phytosterol, and (◆) 1% protein/6% phytosterol. (b) Dynamic interfacial tension measurements of samples containing 1% protein and different concentrations of phytosterols dissolved into MCT; (●) 1% , (▲) 2%, (■) 3%, () 4% phytosterol, (▲) 5%, (◆) 6%

Figure 6. Interfacial tension in weight percentages after 30 min at 60 °C; interfaces are (■) water/(1-6%) phytosterols, (●;0.5-3%) protein/MCT and (◆) 1% protein/(1-6% phytosterols). There is a synergistic effect between the protein and phytosterols adsorbed at the oil-water interface which results in a decrease of interfacial tension in mixed interfaces (represented by dashed lines).

Figure 7. Isotherm fitting to equilibrium interfacial tensions (measured after 30 min at 60 °C). Langmuir and Frumkin isotherms best fit the interfacial tensions for protein (●) and phytosterols (■) respectively. The Langmuir adsorption isotherm was fitted with parameters: adsorption rate constant $b = 5.46 \times 10^7$ l/mmol, Area, $\omega_o = 3.6 \times 10^6$ m²/mol. Frumkin adsorption isotherm was with parameters: adsorption rate constant $b = 9.13 \times 10^{-4}$ l/mmol, Area, $\omega_o = 5 \times 10^4$ m²/mol and interaction parameter $\alpha = 2$.

References

- Acevedo, N. C., & Franchetti, D. (2016). Analysis of co-crystallized free phytosterols with triacylglycerols as a functional food ingredient. *Food Research International*, 85, 104-112. doi:<http://dx.doi.org/10.1016/j.foodres.2016.04.012>
- Andrade, J., & Corredig, M. (2016). Vitamin D3 and phytosterols affect the properties of polyglycerol polyricinoleate (PGPR) and protein interfaces. *Food Hydrocolloids*, 54, Part B, 278-283. doi:<http://dx.doi.org/10.1016/j.foodhyd.2015.10.001>
- Auty, M.A.E., Twomey, M., Guinee, T.P. and Mulvihill, D.M. (2001). Development and application of confocal scanning laser microscopy methods for studying the distribution of fat and protein in selected dairy products. *Journal of Dairy Research*, 68, 417-427.
- Berger, A., Jones, P. J. H., & Abumweis, S. S. (2004). Plant sterols: factors affecting their efficacy and safety as functional food ingredients. *Lipids Health and Disease*, 3(5), 907-919.
- Campbell, I. J. (1989). The role of fat crystals in emulsion stability (pp. 272-282): The Royal Society of Chemistry: Cambridge.
- Campbell, S. D., Goff, & Rousseau, D. (2001). Relating bulk-fat properties to emulsified systems: Characterization of emulsion destabilization by crystallizing fats. In N. Widlak, R. Hartel, & S. Narine (Eds.), *Crystallization and solidification properties of lipids*. (pp. 176-189). Champaign, Illinois: AOCS Press.
- Carden, T. J., Hang, J., Dussault, P. H., & Carr, T. P. (2015). Dietary plant sterol esters must be hydrolyzed to reduce intestinal cholesterol absorption in hamsters. *The Journal of Nutrition*.
- Carr, T. P., Krogstrand, K. L. S., Schlegel, V. L., & Fernandez, M. L. (2009). Stearate-enriched plant sterol esters lower serum LDL cholesterol concentration in normo- and hypercholesterolemic adults. *The Journal of nutrition*, 139(8), 1445-1450.
- Cercaci, L., Rodriguez-Estrada, M. T., Lercker, G., & Decker, E. A. (2007). Phytosterol oxidation in oil-in-water emulsions and bulk oil. *Food Chemistry*, 102(1), 161-167.
- Chen, X.-W., Guo, J., Wang, J.-M., Yin, S.-W., & Yang, X.-Q. (2016). Controlled volatile release of structured emulsions based on phytosterols crystallization. *Food Hydrocolloids*, 56, 170-179. doi:<http://dx.doi.org/10.1016/j.foodhyd.2015.11.035>
- Clifton, P. (2007). *Plant sterols and Stanols as Functional Ingredients in Dairy Products* (M. Saarela Ed. Vol. 2). Oxford, UK Elsevier.
- Corliss, G., Finley, J. W., Basu, H. N., Kincs, F., & Howard, L. (2000).
- Courthaudon, J.-L., Dickinson, E., Matsumura, Y., & Williams, A. (1991). Influence of emulsifier on the competitive adsorption of whey proteins in emulsions. *Food Structure*, 10(2), 1.
- Damodaran, S., Parkin, K. L., & Fennema, O. R. (2007). *Fennema's food chemistry*. Boca Raton, FL: CRC press.
- Dickinson, E. (1999). *Food Emulsions and Foams*. Witney, UK: Elsevier Applied Science Publishers Ltd.
- Drapala, K. P., Auty, M. A. E., Mulvihill, D. M., & O'Mahony, J. A. (2015). Influence of lecithin on the processing stability of model whey protein hydrolysate- based infant formula emulsions. *International Journal of Dairy Technology*, 68(3), 322-333.
- Engel, R., & Schubert, H. (2005). Formulation of phytosterols in emulsions for increased dose response in functional foods. *Innovative Food Science & Emerging Technologies*, 6(2), 233-237.

- Heertje, I. (1993). Microstructural studies in fat research. *Food structure*, 12(1), 10.
- Henson, S., Cranfield, J., & Herath, D. (2010). Understanding consumer receptivity towards foods and non- prescription pills containing phytosterols as a means to offset the risk of cardiovascular disease: an application of protection motivation theory. *International Journal of Consumer Studies*, 34(1), 28-37.
- Herrera, M. L., & Hartel, R. W. (2000). Effect of processing conditions on crystallization kinetics of a milk fat model system. *Journal of the American Oil Chemists' Society*, 77(11), 1177-1188. doi:10.1007/s11746-000-0184-4
- Jandacek, R. J., Webb, M. R., & Mattson, F. H. (1977). Effect of an aqueous phase on the solubility of cholesterol in an oil phase. *Journal of Lipid Research*, 18(2), 203-210.
- Jones, P. J. H., & AbuMweis, S. S. (2009). Phytosterols as functional food ingredients: linkages to cardiovascular disease and cancer. *Current Opinion in Clinical Nutrition & Metabolic Care*, 12(2), 147-151.
- Jones, P. J. H., MacDougall, D. E., Ntanos, F., & Vanstone, C. A. (1997). Dietary phytosterols as cholesterol-lowering agents in humans. *Canadian Journal of Physiology and Pharmacology*, 75(3), 217-227. doi:10.1139/y97-011
- Jumaa, M., & Müller, B. W. (1998). The effect of oil components and homogenization conditions on the physicochemical properties and stability of parenteral fat emulsions. *International Journal of Pharmaceutics*, 163(1), 81-89.
- Keri Marshall, N. (2004). Therapeutic applications of whey protein. *Alternative Medicine Review*, 9(2), 136-156.
- Krog, N., & Larsson, K. (1992). Crystallization at interfaces in food emulsions—a general phenomenon. *Lipid/Fett*, 94(2), 55-57.
- Li, M., Auty, M. A., O'Mahony, J. A., Kelly, A. L., & Brodkorb, A. (2016). Covalent labelling of β -casein and its effect on the microstructure and physico-chemical properties of emulsions stabilised by β -casein and whey protein isolate. *Food Hydrocolloids*.
- Lopez, C., Bourgaux, C., Lesieur, P., & Ollivon, M. (2007). Coupling of time-resolved synchrotron X-ray diffraction and DSC to elucidate the crystallisation properties and polymorphism of triglycerides in milk fat globules. *Le Lait*, 87(4-5), 459-480.
- Maher, P. G., Auty, M. A. E., Roos, Y. H., Zychowski, L. M., & Fenelon, M. A. (2015). Microstructure and lactose crystallization properties in spray dried nanoemulsions. *Food Structure*, 3(0), 11. doi:<http://dx.doi.org/10.1016/j.foostr.2014.10.001>
- Mao, L., Xu, D., Yang, J., Yuan, F., Gao, Y., & Zhao, J. (2009). Effects of small and large molecule emulsifiers on the characteristics of β -carotene nanoemulsions prepared by high pressure homogenization. *Food Technology and Biotechnology*, 47(3), 336-342.
- McClements, D. J. (2004). Protein-stabilized emulsions. *Current Opinion in Colloid & Interface Science*, 9(5), 305-313. doi:<http://dx.doi.org/10.1016/j.cocis.2004.09.003>
- McClements, D. J. (2012). Crystals and crystallization in oil-in-water emulsions: Implications for emulsion-based delivery systems. *Advances in Colloid and Interface Science*, 174, 1-30.
- McClements, D. J. (2015). *Food emulsions: principles, practices, and techniques*. Boca Raton, FL: CRC press.
- Mikes, V., Milat, M.-L., Ponchet, M., Panabières, F., Ricci, P., & Blein, J.-P. (1998). Elicitins, Proteinaceous Elicitors of Plant Defense, Are a New Class of Sterol Carrier Proteins. *Biochemical and Biophysical Research Communications*, 245(1), 133-139. doi:<https://doi.org/10.1006/bbrc.1998.8341>
- Möbius, D., Miller, R., & Fainerman, V. B. (2001). *Surfactants: chemistry, interfacial properties, applications* (Vol. 13): Elsevier.

- Moruisi, K. G., Oosthuizen, W., & Opperman, A. M. (2006). Phytosterols/stanols lower cholesterol concentrations in familial hypercholesterolemic subjects: a systematic review with meta-analysis. *Journal of the American College of Nutrition*, 25(1), 41-48.
- Norton, J. E., & Fryer, P. J. (2012). Investigation of changes in formulation and processing parameters on the physical properties of cocoa butter emulsions. *Journal of Food Engineering*, 113(2), 329-336.
- Ostlund, R. E. (2002). Phytosterols in human nutrition. *Annual Review of Nutrition*, 22(1), 533-549.
- Ostlund, R. E., Spilburg, C. A., & Stenson, W. F. (1999). Sitostanol administered in lecithin micelles potentially reduces cholesterol absorption in humans. *The American Journal of Clinical Nutrition*, 70(5), 826-831.
- Pouteau, E. B., Monnard, I. E., Piguet-Welsch, C., Groux, M. J. A., Sagalowicz, L., & Berger, A. (2003). Non-esterified plant sterols solubilized in low fat milks inhibit cholesterol absorption. *European Journal of Nutrition*, 42(3), 154-164. doi:10.1007/s00394-003-0406-6
- Pradines, V., Krägel, J. r., Fainerman, V. B., & Miller, R. (2008). Interfacial properties of mixed β -lactoglobulin–SDS layers at the water/air and water/oil interface. *The Journal of Physical Chemistry B*, 113(3), 745-751.
- Reddy, S., & Ghosh, P. (2010). Adsorption and coalescence in mixed surfactant systems: Water–hydrocarbon interface. *Chemical Engineering Science*, 65(14), 4141-4153.
- Rosen, M. J., & Hua, X. Y. (1982). Surface concentrations and molecular interactions in binary mixtures of surfactants. *Journal of Colloid and Interface Science*, 86(1), 164-172.
- Rosen, M. J., & Zhou, Q. (2001). Surfactant–surfactant interactions in mixed monolayer and mixed micelle formation. *Langmuir*, 17(12), 3532-3537.
- Rossi, L., ten Hoorn, J. W. S., Melnikov, S. M., & Velikov, K. P. (2010). Colloidal phytosterols: synthesis, characterization and bioaccessibility. *Soft Matter*, 6(5), 928-936.
- Rouimi, S., Schorsch, C., Valentini, C., & Vaslin, S. (2005). Foam stability and interfacial properties of milk protein–surfactant systems. *Food Hydrocolloids*, 19(3), 467-478. doi:<http://dx.doi.org/10.1016/j.foodhyd.2004.10.032>
- Rousseau, D. (2000). Fat crystals and emulsion stability — a review. *Food Research International*, 33(1), 3-14. doi:[http://dx.doi.org/10.1016/S0963-9969\(00\)00017-X](http://dx.doi.org/10.1016/S0963-9969(00)00017-X)
- Rubingh, D. N. (1979). Mixed micelle solutions *Solution chemistry of surfactants* (pp. 337-354): Springer.
- Salager, J., Morgan, J., Schechter, R., Wade, W., & Vasquez, E. (1979). Optimum formulation of surfactant/water/oil systems for minimum interfacial tension or phase behavior. *Society of Petroleum Engineers Journal*, 19(02), 107-115.
- Santas, J., Codony, R., & Rafecas, M. (2013). Phytosterols: Beneficial Effects. In K. G. Ramawat & J.-M. Mérillon (Eds.), *Natural Products* (pp. 3437-3464): Springer Berlin Heidelberg.
- Spaepen, F. (1994). Homogeneous Nucleation and the Temperature Dependence of the Crystal-Melt Interfacial Tension. In H. Ehrenreich & D. Turnbull (Eds.), *Solid State Physics* (Vol. 47, pp. 1-32): Academic Press.
- Sünder, A., Scherze, I., & Muschiolik, G. (2001). Physico-chemical characteristics of oil-in-water emulsions based on whey protein–phospholipid mixtures. *Colloids and Surfaces: Biointerfaces*, 21(1–3), 75-85. doi:[http://dx.doi.org/10.1016/S0927-7765\(01\)00186-2](http://dx.doi.org/10.1016/S0927-7765(01)00186-2)
- Thivilliers, F., Laurichesse, E., Saadaoui, H., Leal-Calderon, F., & Schmitt, V. (2008). Thermally induced gelling of oil-in-water emulsions comprising partially crystallized droplets: the impact of interfacial crystals. *Langmuir*, 24(23), 13364-13375.

- Toro- Vazquez, J. F., Rangel- Vargas, E., Dibildox- Alvarado, E., & Charó- Alonso, M. A. (2005). Crystallization of cocoa butter with and without polar lipids evaluated by rheometry, calorimetry and polarized light microscopy. *European Journal of Lipid Science and Technology*, 107(9), 641-655.
- Truong, T., Bansal, N., Sharma, R., Palmer, M., & Bhandari, B. (2014). Effects of emulsion droplet sizes on the crystallisation of milk fat. *Food Chemistry*, 145(0), 725-735. doi:<http://dx.doi.org/10.1016/j.foodchem.2013.08.072>
- Waninge, R., Walstra, P., Bastiaans, J., Nieuwenhuijse, H., Nylander, T., Paulsson, M., & Bergenståhl, B. (2005). Competitive Adsorption between β -Casein or β -Lactoglobulin and Model Milk Membrane Lipids at Oil–Water Interfaces. *Journal of Agricultural and Food Chemistry*, 53(3), 716-724. doi:10.1021/jf049267y
- Widlak, N., Hartel, R. W., & Narine, S. (2001). *Crystallization and solidification properties of lipids*. Champaign, IL: The American Oil Chemists Society.
- Wüstneck, R., Krägel, J., Miller, R., Wilde, P. J., & Clark, D. C. (1996). The adsorption of surface-active complexes between β -casein, β -lactoglobulin and ionic surfactants and their shear rheological behaviour. *Colloids and Surfaces A: Physicochemical and Engineering Aspects*, 114, 255-265.
- Zawistowski, J. (2010). 17 Tangible health benefits of phytosterol functional foods. *Functional Food Product Development*, 2.
- Zhou, Q., & Rosen, M. J. (2003). Molecular interactions of surfactants in mixed monolayers at the air/aqueous solution interface and in mixed micelles in aqueous media: the regular solution approach. *Langmuir*, 19(11), 4555-4562.
- Zychowski, L. M., Logan, A., Augustin, M. A., Kelly, A. L., O'Mahony, J. A., Conn, C. E., & Auty, M. A. (2018). Phytosterol crystallisation within bulk and dispersed triacylglycerol matrices as influenced by oil droplet size and low molecular weight surfactant addition. *Food Chemistry*, 264, 24-33.
- Zychowski, L. M., Logan, A., Augustin, M. A., Kelly, A. L., Zabara, A., O'Mahony, J. A., . . . Auty, M. A. (2016). Effect of Phytosterols on the Crystallization Behavior of Oil-in-Water Milk Fat Emulsions. *Journal of Agricultural and Food Chemistry*, 64(34), 6546–6554.

Figures

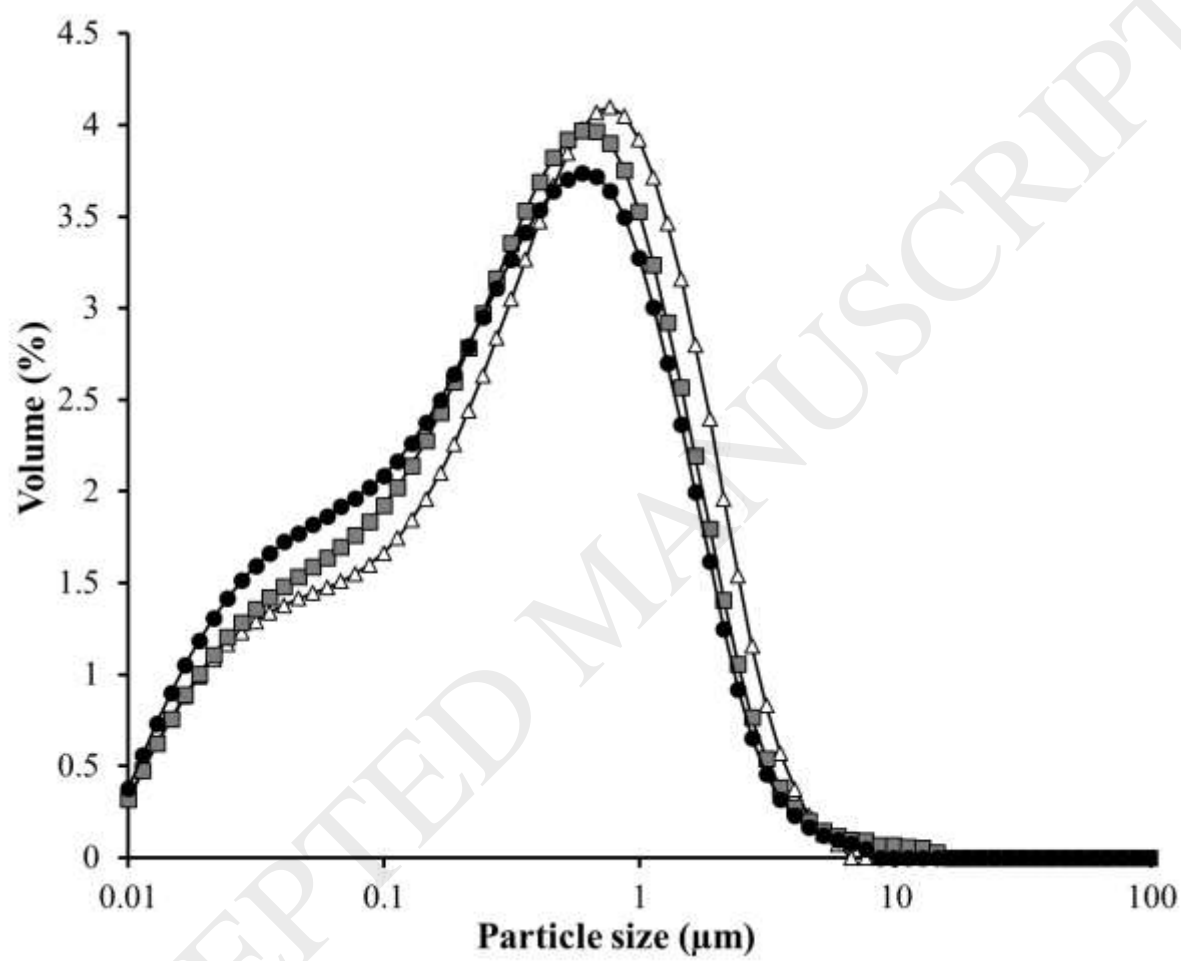


Figure 1

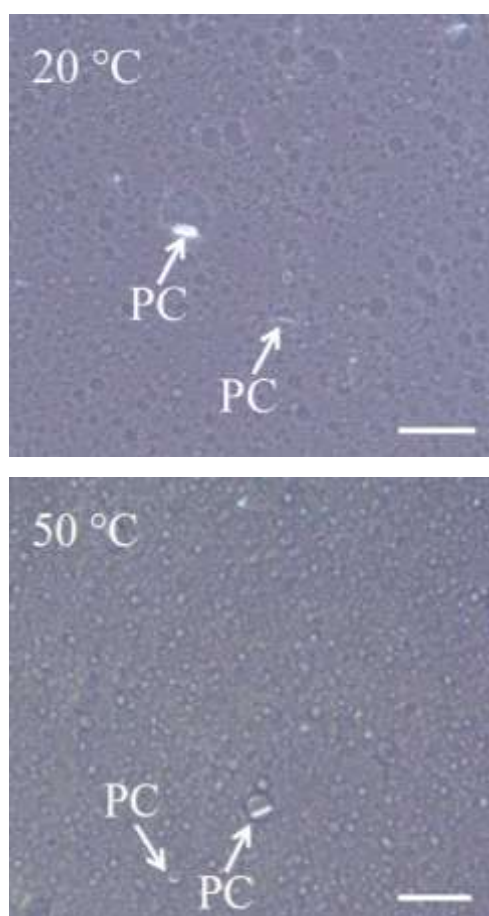


Figure 2

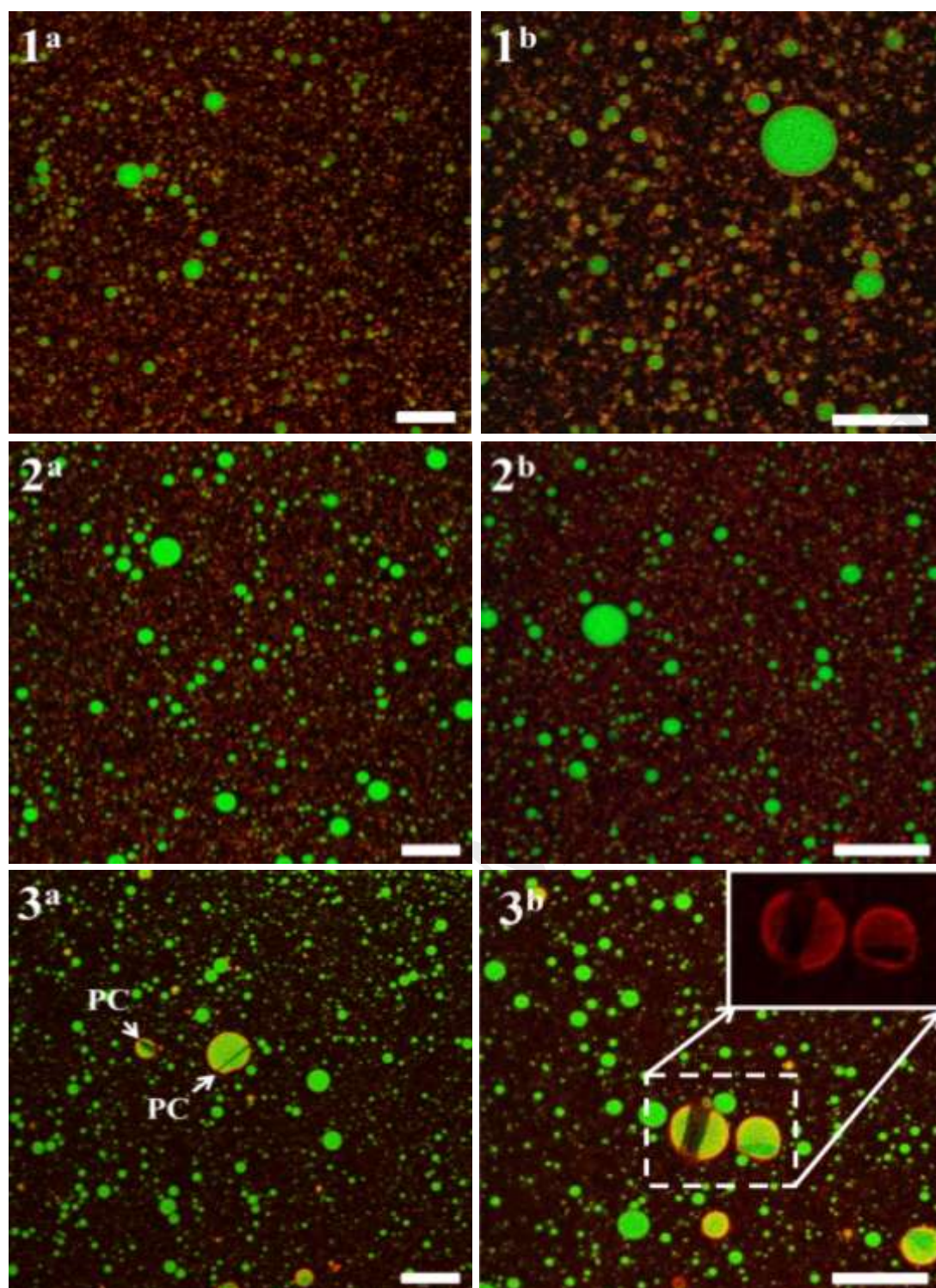


Figure 3

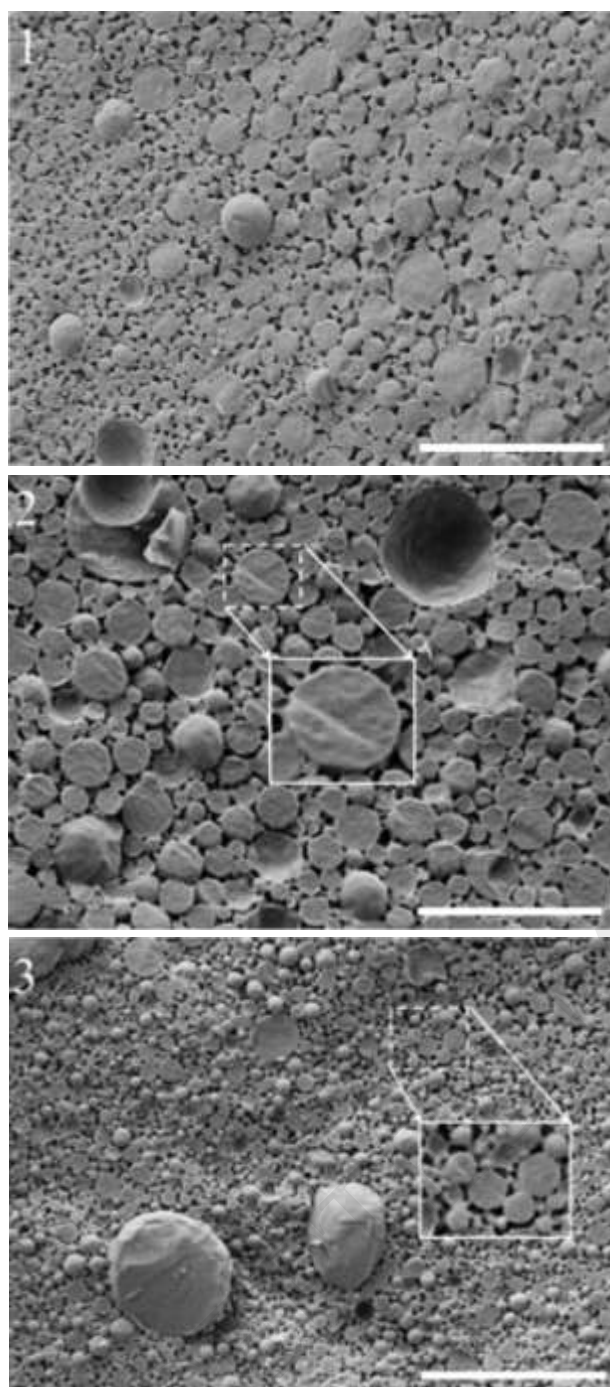


Figure 4

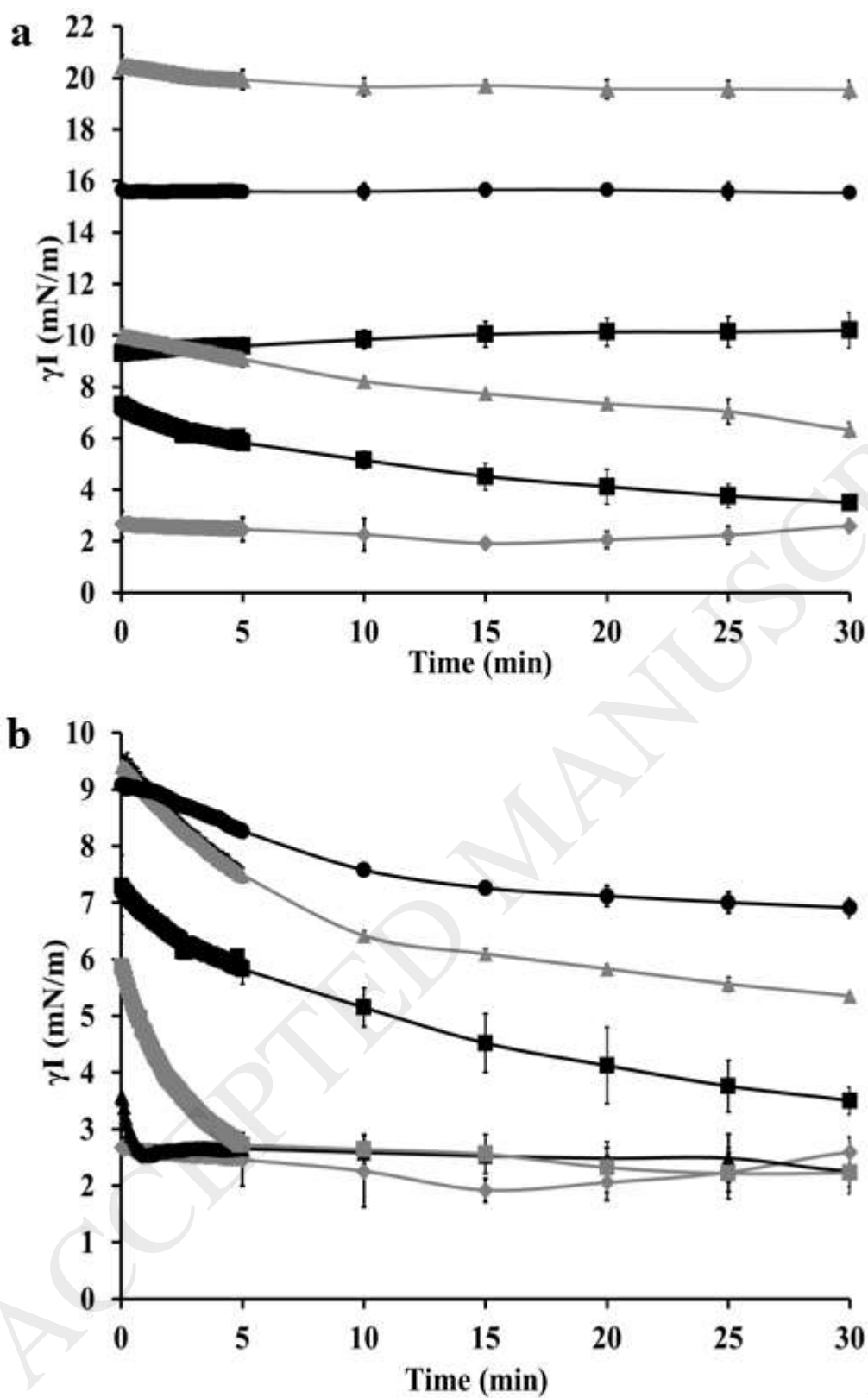


Figure 5

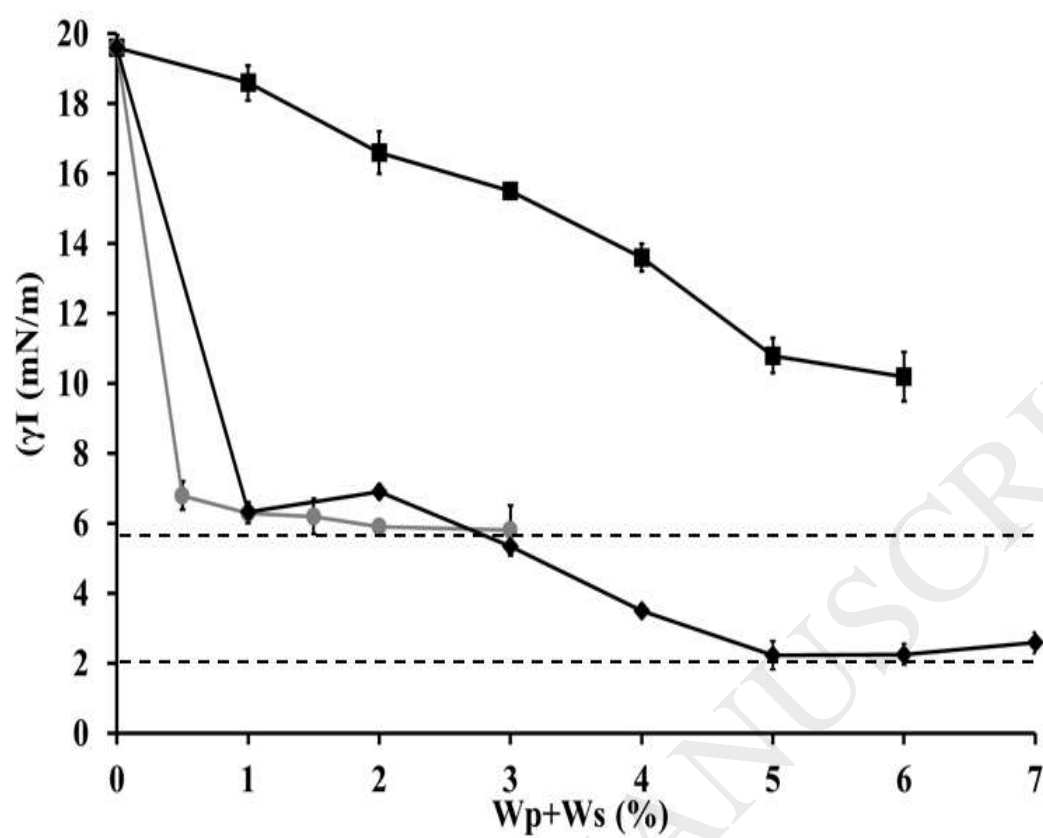


Figure 6

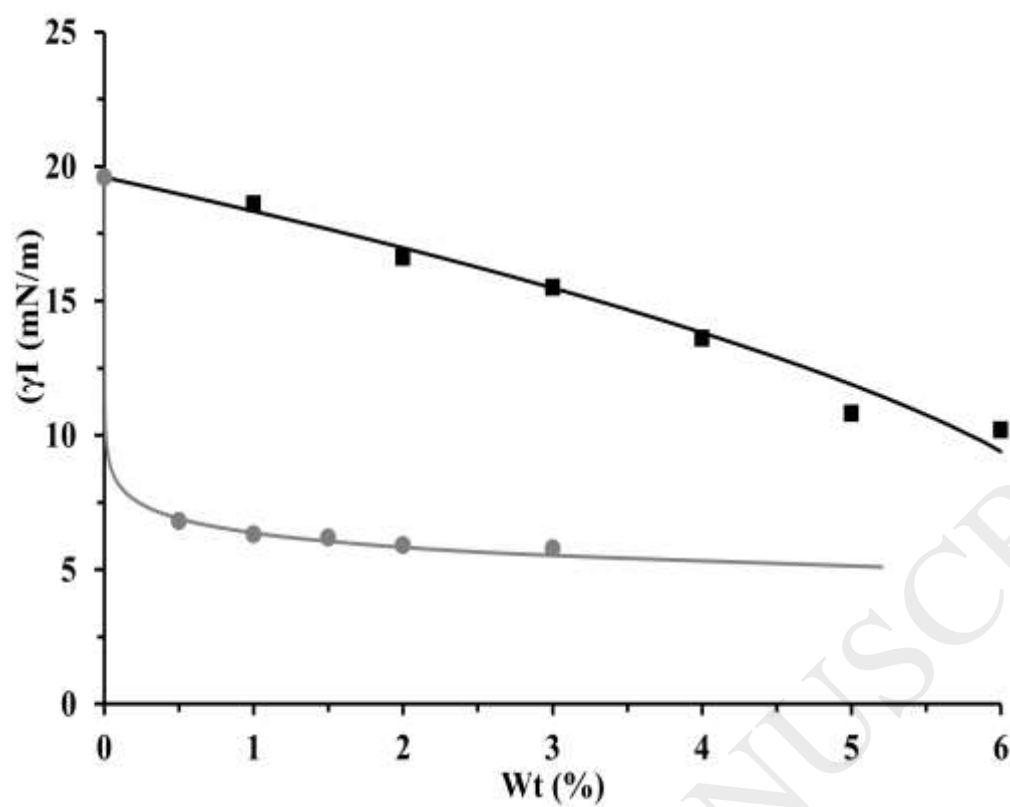


Figure 7